Inorganic Chemistry

pubs.acs.org/IC Article

Reduction of Rare-Earth Metal Complexes Induced by γ Irradiation

William N. G. Moore, Jessica R. K. White, Justin C. Wedal, Filipp Furche,* and William J. Evans*



Cite This: Inorg. Chem. 2022, 61, 17713-17718



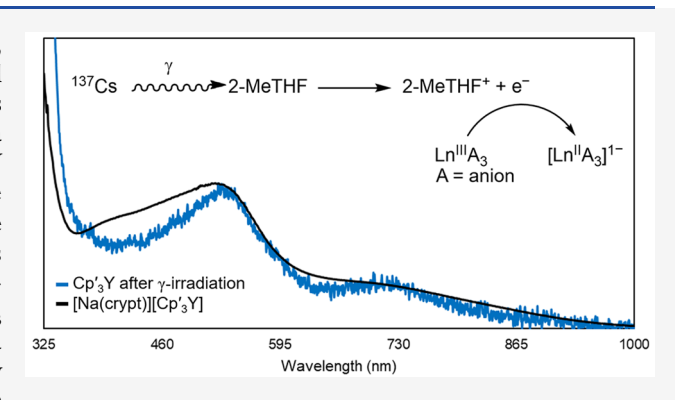
ACCESS

Metrics & More

Article Recommendations

Supporting Information

ABSTRACT: The utility of *γ* irradiation for generating unstable, low oxidation state molecular species containing rare-earth metal ions in frozen solution has been examined. The method was evaluated by irradiating Ln(III) precursors (Ln = Sc, Y, and La) in a solid matrix of 2-methyltetrahydrofuran at 77 K with a 700 keV 137 Cs source to generate free electrons capable of reducing the Ln(III) species. These experiments yielded EPR and UV–visible spectroscopic data that matched those of the known Ln(II) species $[(C_5H_4SiMe_3)_3Y^{II}]^{1-}$, $[(C_5H_4SiMe_3)_3La^{II}]^{1-}$, and $\{Sc^{II}[N-(SiMe_3)_2]_3\}^{1-}$. Irradiation of the La(III) complex La^{III}[N(SiMe₃)₂]₃ by this method gave EPR and UV–visible absorption spectra consistent with $\{La^{II}[N(SiMe_3)_2]_3\}^{1-}$, a species that had previously eluded preparation by chemical reduction. Specifically, the



irradiation product exhibited an axial EPR spectrum split into eight lines by the I = 7/2 ¹³⁹La nucleus ($g_{\perp} = 1.98$, $g_{\parallel} = 2.06$, $A_{\text{ave}} = 519.1$ G). The UV-visible absorption spectrum contains broad bands centered at 390 and 670 nm that are consistent with a La(II) ion in a trigonal ligand environment based on time-dependent density functional theory which qualitatively reproduces the observed spectrum. Additionally, the rate of formation of the $[(C_5H_4\text{SiMe}_3)_3Y^{\text{II}}]^{1-}$ species during the irradiation of $(C_5H_4\text{SiMe}_3)_3Y^{\text{III}}$ was monitored by measuring the concentration via UV-visible spectroscopy over time to provide data on the rate at which a molecular species is reduced in a glass via γ irradiation.

■ INTRODUCTION

One of the major advances in the chemistry of the rare-earth elements (Ln), that is, scandium, yttrium, and the lanthanides, was the discovery that the +2 oxidation state was accessible not only for Eu(II), Yb(II), Sm(II), Tm(II), Dy(II), and Nd(II)¹⁻⁵ but also for all the other rare-earth metals except radioactive promethium.6-9 The new Ln(II) ions were frequently generated in trigonal ligand environments in which a dz^2 orbital was populated to give $3d^1$ (Sc), $4d^1$ (Y), and 4fⁿ5d¹ (lanthanides) electron configurations. 5,9,10 These new Ln(II) species are of interest not only due to their highly reducing reactivity 11-16 but also due to their physical properties. 17-19 Synthesis of complexes of the new Ln(II) ions generally requires sub-ambient temperatures and short reaction times. Although many examples of 4f'5d1 Ln(II) complexes are now known, reduction of some Ln(III) precursors with alkali metals yields only fleeting color changes and the Ln(II) products have evaded definitive characterization. 20-22 Therefore, it is of interest to explore alternative methods for generating Ln(II) complexes.

Alternative reduction methods were also desirable because the discovery of molecular complexes of the new Ln(II) ions raised the question about the potential availability of molecular complexes containing Ln(I) ions. ^{23,24} Since crystallographically characterized Ln(0) complexes, Ln(1,3,5-tri–tert-butylbenzene)₂ for Ln = Sc, Y, Gd, and Ho, are already known^{25–27}

as well as an example of a Sc(I) compound, $[\{(\eta^5 - P_3C_2^tBu_2)Sc\}_2(\mu-\eta^6:\eta^6-P_3C_3^tBu_3)]^{28}$ the pursuit of molecular Ln(I) coordination compounds for other rare-earth metals is an intriguing target.

In fact, γ irradiation was previously used in 1966 to provide evidence for the formation of Sm(I) ions in a KCl matrix. By subjecting single crystals of Sm(II) doped into a KCl matrix grown from a melt phase to γ irradiation on the order of 2–20 Mrad (20–200 Gy), data were generated that suggested reduction of Sm(II) to Sm(I).²⁹ The γ irradiation method was also applied in the 1960s to Ln(III) ions doped into MF₂ matrices (M = Ca, Sr, Ba); the resulting spectra were assigned to Ln(II) ions for the whole lanthanide series.^{30,31} Subsequent studies have shown that γ irradiation of glasses containing Sm(III) ions results in reduction to Sm(II) ions based on UV–visible spectroscopy.^{32,33} These glasses are typically prepared using a conventional melt/quench process and use Sm₂O₃ as the samarium starting material. Upon γ irradiation of the glasses using dosages on the order of 3–20 Mrad (30–200

Received: August 9, 2022 Published: October 25, 2022





Gy), UV-visible spectroscopy usually shows a single peak around 320 nm corresponding to a 4f-5d transition typical of a Sm(II) ion. ³²

Since these previous crystal lattice and glassy matrix rareearth metal studies required high-temperature melt/quench techniques to prepare the precursors, they were not extendable to molecular species of lower thermal stability. However, γ -irradiation-based cryoreduction has previously been successful in bioinorganic systems, ^{34–39} and thus the extension to molecular rare-earth metal complexes seemed reasonable. In this study, we report on the viability of γ irradiation of frozen solutions of molecular rare-earth metal species as a method to generate reactive Ln(II) species. These preliminary studies demonstrate the viability of the method and identify a new La(II) complex previously inaccessible in solution. Sc (I=7/2), Y (I=1/2), and La (I=7/2) were the rare-earth metals chosen for this study since their d¹ Ln(II) ions exhibit definitive EPR spectra due to coupling to their nuclear spins.

■ EXPERIMENTAL SECTION

All manipulations and syntheses described below were conducted with the rigorous exclusion of air and water using standard Schlenk line and glovebox techniques under an argon atmosphere. Anhydrous 2-Methyltetrahydrofuran (2-MeTHF) was transferred onto dry 3 Å molecular sieves and degassed in vacuo until solvent evaporation was observed. UV—visible absorbance spectra were collected on an Agilent Cary 60 UV—vis. EPR spectra were collected using the X-band frequency (9.3–9.8 GHz) on a Bruker EMX spectrometer equipped with an ER4119HS-W1 microwave bridge. $Sc^{III}(NR_2)_3,^{40}$ $Cp_3^{\prime}Y^{III},^{7}$ $Cp_3^{\prime}La^{III},^{41}$ and $La^{III}(NR_2)_3,^{40}$ were synthesized via literature procedures $(Cp^{\prime}=C_5H_4SiMe_3,~R=SiMe_3).$

General γ Irradiation Procedure. In an argon-filled glovebox, 0.3 mL of a 0.05–0.5 M solution of the Ln(III) starting material in 2-MeTHF was transferred by pipet into an EPR tube. The tube was sealed with a rubber septum, removed from the inert atmosphere glovebox, and further sealed by wrapping with parafilm. The tube was then *rapidly* (within one second) inserted into a Dewar filled with liquid nitrogen because slow insertion led to poor solvent glassing and inhibited characterization attempts. The Dewar was then exposed to 700 keV γ irradiation from a ¹³⁷Cs source in the UCI Nuclear Reactor Facility (see Figure S1 for a brief workflow diagram). *Caution!* γ irradiation is an ionizing form of electromagnetic irradiation that may cause biological damage. Studies must be conducted using appropriate radiological safety equipment and procedures. Following irradiation, continuous wave, X-band EPR spectra were collected at 77 K in perpendicular mode.

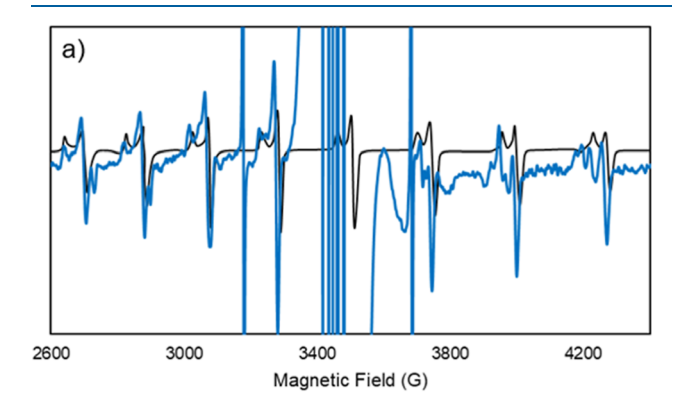
The following procedure was utilized to collect UV—visible spectra on the irradiated samples. A finger Dewar was half-filled with liquid nitrogen and clamped so that the finger was as close as possible to the detection slit of an Agilent Cary 60 UV—visible spectrophotometer while remaining vertical (see Figure S2 for positioning and diagram). The finger was subjected to a stream of nitrogen gas from a high-pressure cylinder to prevent condensation of atmospheric water. The sample EPR tube was inserted into the finger Dewar, and a spectrum was collected at a speed of 300 nm/min. Two more spectra were collected sequentially using the same rate, and the spectra were averaged. The final spectrum was obtained by subtracting the average spectrum of irradiated 2-MeTHF.

RESULTS AND DISCUSSION

 γ Irradiation of 2-MeTHF. A control sample with no added Ln(III) compound was exposed to 16 h of γ irradiation (about 2 Mrad or 20 Gy total). EPR spectroscopy at 77 K revealed an intense isotropic signal ($g_{\rm iso} = 2.002$; see Figure S3) associated with irradiated organic solvents. UV-visible spectroscopy of the sample showed a broad absorption

increasing beyond the 1000 nm limit of the spectrometer (see Figure S4), which is consistent with known irradiated samples of 2-MeTHF, $\lambda_{\text{max}} = 2150 \text{ nm}$ ($\varepsilon = 3.9 \times 10^4 \text{ M}^{-1}$ cm⁻¹).⁴² Attempts to minimize the organic radical EPR signal in irradiated rare-earth metal samples without perturbing the Ln(II) signal (see below) via photobleaching and annealing at 195 and 174 K were unsuccessful: only a weak organic radical signal was observed and no signal from the Ln(II) ion was observed. Attempts to subtract the EPR spectrum of irradiated 2-MeTHF collected after identical irradiation periods were also unsuccessful. On the other hand, UV-visible absorption spectroscopy allowed for relatively simple background subtraction. Radical absorption could be subtracted in a straightforward manner by irradiating samples of pure 2-MeTHF along with the rare-earth samples of interest for the same amount of time and subtracting the irradiated solvent

γ Irradiation of Ln(III) Compounds with Known Ln(II) Analogues. The Ln(III) compounds $Sc^{III}(NR_2)_3$, $Cp_3'Y^{III}$, and $Cp_3'La^{III}$ ($R=SiMe_3$, $Cp'=C_5H_4SiMe_3$) were chosen to probe the viability of the method since their corresponding Ln(II) compounds have been chemically isolated, exhibit distinctive EPR spectra, and have UV-visible spectra with distinctive absorptions. 7,10,12,21 The known EPR spectra of $[Sc^{II}(NR_2)_3]^{1-12}$ and $[Cp_3'La^{II}]^{1-10}$ were clearly discernible even in the presence of the irradiated solvent peak, Figure 1, Table 1, but the hyperfine coupling (A) of $[Cp_3'Y^{II}]^{1-}$ was unresolved under these conditions (Figure S5). However, the UV-visible spectra for the Ln(II) species generated from γ irradiation of these compounds in all cases were consistent



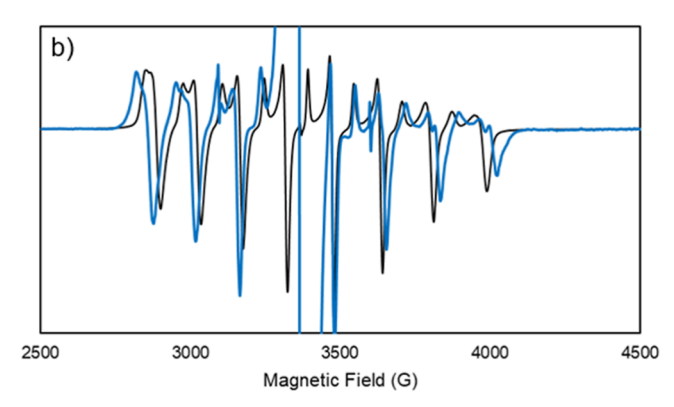


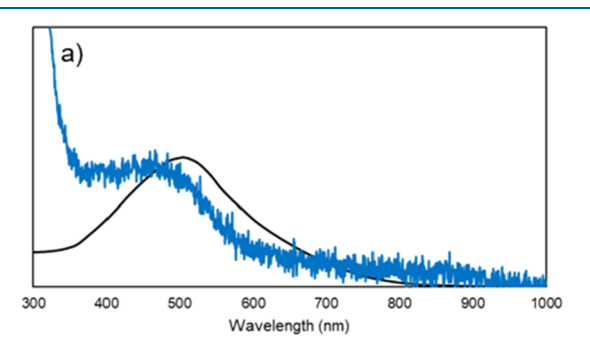
Figure 1. Normalized EPR spectroscopic comparison of $[Ln^{II}A_3]^{1-}$ species (A = anion) generated from the γ irradiation procedure (blue) and chemical reduction (black): (a) $[Sc^{II}(NR_2)_3]^{1-}$; (b) $[Cp_3'La^{II}]^{1-}$.

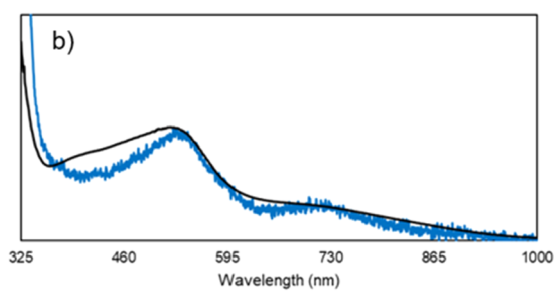
Table 1. Comparison of Spectroscopic Data of $[Ln^{II}A_3]^{1-}$ Species (A = Anion) Generated from the γ Irradiation Procedure (a) and Chemical Reduction (b), Where crypt = 2.2.2-Cryptand

	λ_{\max} (nm)	g_{\perp}	g_{\parallel}	(G, MHz)
(a) $[Sc^{II}(NR_2)_3]^{1-}$	500	1.96	2.00	225.7, 625.3
(b) $[K(crypt)][Sc^{II}(NR_2)_3]^{12}$	516	1.964	1.997	225, 622.6
(a) $[Cp_3'Y^{II}]^{1-}$	530, 700			
(b) [Na(crypt)][Cp' ₃ Y ^{II}] ²¹	390, 530, 700	1.99	2.00	36.6, 100.9
(a) $[Cp_3'La^{II}]^{1-}$	310, 425, 567, 692	1.96	1.98	164.2, 450.9
(b) [K(crypt)][Cp ₃ 'La ^{II}] ¹⁰	310, 433, 502, 554, 692	1.96	1.99	155.4, 427.3

with those generated from chemical reduction, Figure 2, Table 1.

 γ Irradiation of La^{III}(NR₂)₃. Given the observed consistency between spectroscopic data obtained after γ irradiation and chemical reduction experiments with the compounds above, the characterization of a new Ln(II) species was attempted. Specifically, generation of $[La^{II}(NR_2)_3]^{1-}$ was





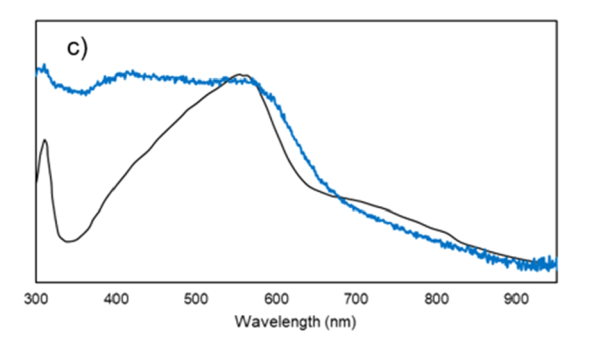


Figure 2. Normalized UV–visible spectroscopic comparison of $[Ln^{II}A_3]^{1-}$ species (A = anion) generated from the γ irradiation procedure (blue) and chemical reduction (black): (a) $[Sc^{II}(NR_2)_3]^{1-}$; (b) $[Cp_3'Y^{II}]^{1-}$; (c) $[Cp_3'La^{II}]^{1-}$.

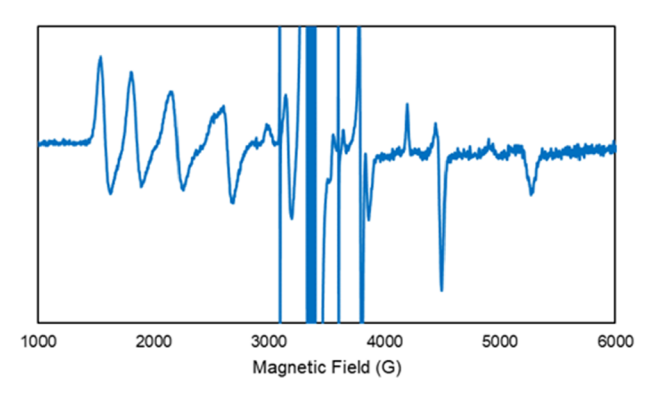
pursued since it is a species that previously has not been observable in chemical reductions. Using the general γ irradiation procedure outlined above, La^{III}(NR₂)₃ (69 mg, 0.11 mmol) was dissolved in 0.3 mL of 2-MeTHF and exposed to 12 h of γ irradiation for a total of about 1.5 Mrad (150 Gy). The EPR spectrum of the resulting sample at 77 K exhibited the characteristic isotropic signal for the radical formed by the irradiation of 2-MeTHF ($g_{iso} = 2.002$) as well as an eight line signal (g_{\perp} = 1.98, g_{\parallel} = 2.06, A_{ave} = 504.3 G = 1420.4 MHz) consistent with an unpaired electron in an axial environment coupled to a 139La nucleus (see Figure 3). The hyperfine coupling constant is about 3 times greater than that of $[Cp_3'La^{II}]^{1-}$ ($A_{ave} = 164.4$ G), which is similar in magnitude to the differences observed between $[Y^{II}(NR_2)_3]^{1-}$ (A=110.0 G)⁴² and $[Cp_3'Y^{II}]^{1-}$ (A=36.6 G). The UV-visible spectrum of the sample contains distinct bands at 390 and 670 nm. The UV-visible spectrum is consistent with metal-based $5d \rightarrow 6p$ transitions observed for other $[Ln^{II}(NR_2)_3]^{1-}$ complexes with 4f'5d1 electron configurations. 22,43,44

Theoretical Studies on $[La^{II}(NR_2)_3]^{1-}$. Electronic structure calculations of the putative La(II) species [La^{II}(NR₂)₃]¹⁻ were performed at the density functional level of theory using the TPSSh hybrid meta-generalized gradient density functional⁴⁵ with the D3 dispersion correction^{46,47} and the resolution of the identity approximation.⁴⁸ A scalar relativistic effective core potential with the def2-TZVP basis set⁴⁹ was used for lanthanum, and the polarized split-valence basis sets def2-SV(P) were used for other atoms. 50 The continuum solvent model COSMO⁵¹ was used with parameters for THF (dielectric constant $\varepsilon = 7.52$, refractive index $R_{\rm ind} = 1.41$).⁵² TDDFT calculations were performed with an additional diffuse p primitive added to the La basis set, which was necessary to accurately simulate the absorption spectrum. 44,53-55 All calculations were performed with the TURBOMOLE package V7.4.1.56,57 Complete details can be found in the Supporting Information.

Structure optimizations were initiated from the optimized structure of $[Gd(NR_2)_3]^{1-44}$ by replacing Gd with La. The resulting ground-state geometry of $[La^{II}(NR_2)_3]^{1-}$ had C_3 symmetry. The electronic configuration was consistent with a $(5dz^2)^1$ configuration, with the highest occupied molecular orbital (HOMO) having significant $5dz^2$ -character with 6s admixture, Figure 4. These results are consistent with previous studies on $[Ln^{II}(NR_2)_3]^{1-}$ complexes 22,44 and other $[La^{II}A_3]^{1-}$ (A = anion) species. 9,12,55

The simulated UV–visible spectrum of $[La^{II}(NR_2)_3]^{1-}$ qualitatively matches the spectrum obtained by γ irradiation studies, Figure 2. Strong transitions between 650 and 700 nm are metal-based with 5d \rightarrow 6p character, consistent with previous studies on $[Gd^{II}(NR_2)_3]^{1-}$.⁴⁴ Hence, it appears that γ irradiation of $La^{III}(NR_2)_3$ generated $[La^{II}(NR_2)_3]^{1-}$, which has been difficult to generate by chemical reduction methods.

Rate of Formation of $[Cp_3'Y^{II}]^{1-}$. Given the particularly good agreement between the electronic absorption spectrum of $[Cp_3'Y^{II}]^{1-}$ prepared by either chemical reduction or γ irradiation and the fact that the spectra of many different salts of $[Cp_3'Y^{II}]^{1-}$ are identical regardless of the cation present, the absorption at 530 nm of $[Cp_3'Y^{II}]^{1-}$ was used to monitor the growth of Y(II) with increasing dosages of γ irradiation. A path length of 0.3 cm was determined experimentally using fluorenone as a known standard (see Figure S6). Additionally, different starting concentrations (0.075 vs 0.15 M) of the Y(III) complex $Cp_3'Y^{III}$ were used



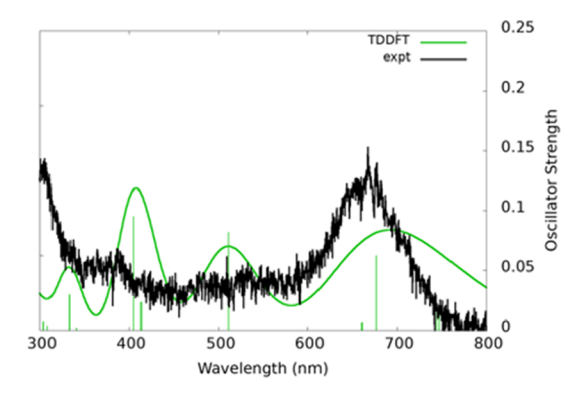


Figure 3. EPR (left) and UV–visible absorbance (right) spectroscopic characterization of the species generated upon γ irradiation of La^{III}(NR₂)₃. The simulated UV–visible spectrum is shown in green (right) with computed time-dependent density functional theory (TDDFT) oscillator strengths shown as vertical lines. A Gaussian line broadening of 0.15 eV was applied, and the spectrum was empirically blue-shifted by 0.30 eV.

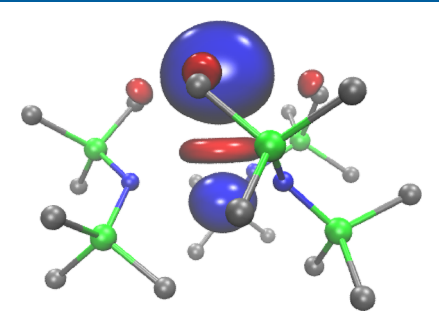


Figure 4. Calculated $5dz^2$ -like HOMO ($\varepsilon = -1.439$ eV) of $[La^{II}(NR_2)_3]^{1-}$ plotted with a contour value of 0.05.

to determine if this affected the rate of Y(II) formation. The data, recorded in triplicate, are plotted in Figure 5. Though the

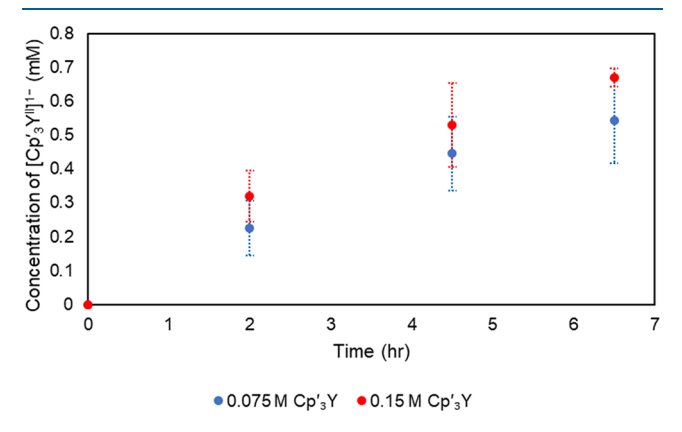


Figure 5. Growth of $[Cp'_3Y^{II}]^{1-}$ over time from γ irradiation of two different initial concentrations of Cp'_3Y^{III} .

relatively large uncertainties prohibit definitive kinetic analysis, there is clearly a growth of Y(II) over time. This concentration study showed that after 6.5 h of irradiation, <1% of $Cp_3'Y^{III}$ has been reduced. Further studies aimed at converting the bulk may benefit from utilizing a higher dosage setup.

CONCLUSIONS

 γ irradiation of $Sc^{III}(NR_2)_3$ and $Cp_3'La^{III}$ yielded 77 K EPR and UV–visible absorption spectra indicative of reduction to the highly reactive Ln(II) complexes, $\left[Sc^{II}(NR_2)_3\right]^{1-}$ and $\left[Cp_3'La^{II}\right]^{1-}$. A significant obstacle for characterization by EPR spectroscopy is the intense signal associated with the

organic radical formed from irradiating 2-MeTHF. This obscured the EPR signal of the Cp₃'Y^{III} irradiation product, but $[Cp_3'Y^{II}]^{1-}$ could be identified by UV—visible spectroscopy. In general, by studying species containing rare-earth metals with large nuclear spins (I=7/2) and large coupling constants, the Ln(II) species formed by irradiation can be detected via EPR spectroscopy. This demonstrates the viability of the γ irradiation reductive technique with molecular rare-earth metal species. Extension of this method to $La^{III}(NR_2)_3$ led to spectroscopic characterization of $[La^{II}(NR_2)_3]^{1-}$ for the first time and shows that this method can be used to demonstrate the existence of species not yet isolable by chemical reduction. Hence, γ irradiation should be more widely considered for generating highly reactive molecular species when the appropriate spectroscopic assessments can be made.

ASSOCIATED CONTENT

Supporting Information

The Supporting Information is available free of charge at https://pubs.acs.org/doi/10.1021/acs.inorgchem.2c02857.

EPR and UV–visible spectra of 2-MeTHF after γ irradiation, diagram of the UV–visible data collection setup, computational details, and optimized coordinates (PDF)

AUTHOR INFORMATION

Corresponding Authors

Filipp Furche — Department of Chemistry, University of California, Irvine, California 92697-2025, United States; orcid.org/0000-0001-8520-3971; Email: filipp.furche@uci.edu

William J. Evans — Department of Chemistry, University of California, Irvine, California 92697-2025, United States; orcid.org/0000-0002-0651-418X; Email: wevans@uci.edu

Authors

William N. G. Moore — Department of Chemistry, University of California, Irvine, California 92697-2025, United States; orcid.org/0000-0001-5074-9341

Jessica R. K. White — Department of Chemistry, University of California, Irvine, California 92697-2025, United States

Justin C. Wedal — Department of Chemistry, University of California, Irvine, California 92697-2025, United States;

orcid.org/0000-0003-0437-8601

Complete contact information is available at: https://pubs.acs.org/10.1021/acs.inorgchem.2c02857

Notes

The authors declare the following competing financial interest(s): Principal Investigator Filipp Furche has an equity interest in TURBOMOLE GmbH. The terms of this arrangement have been reviewed and approved by the University of California, Irvine, in accordance with its conflict of interest policies.

ACKNOWLEDGMENTS

We thank the U.S. National Science Foundation for support of the experimental parts of this research under CHE-2154255 (to W.J.E.) and the theoretical parts under CHE-2102568 (to F.F.). The authors are extremely grateful to Dr. Tro Babikian and John Keffer with the UCI Nuclear Facility for their help using the γ irradiation source and refilling the Dewar as needed. Additionally, the authors would like to thank Prof. Michael T. Green for helping assembling the 77 K UV—visible absorption spectroscopy setup.

REFERENCES

- (1) Morss, L. R. Thermochemical Properties of Yttrium, Lanthanum, and the Lanthanide Elements and Ions. *Chem. Rev.* **1976**, *76*, 827–841.
- (2) Nugent, L. J.; Baybarz, R. D.; Burnett, J. L.; Ryan, J. L. Electron-Transfer and f→d Absorption Bands of Some Lanthanide and Actinide Complexes and the Standard (III-IV) Oxidation Potentials for Each Member of the Lanthanide and Actinide Series. *J. Inorg. Nucl. Chem.* 1971, 33, 2503–2530.
- (3) Bochkarev, M. N. Molecular Compounds of "New" Divalent Lanthanides. Coord. Chem. Rev. 2004, 248, 835-851.
- (4) Nief, F. Handbook on the Physics and Chemistry of Rare Earths, Gschneidner, K. A., Jr., Bunzli, J.-C. G., Pecharsky, V. K., Eds.; Elsevier: North-Holland, Amsterdam, 2010; Vol. 40, Chapter 246.
- (5) Woen, D. H.; Evans, W. J. Expanding the +2 Oxidation State of the Rare-Earth Metals, Uranium, and Thorium in Molecular Complexes. In *Handbook on the Physics and Chemistry of Rare Earths*; Elsevier B.V., 2016, Chapter 293; Vol. 50, pp 337–394.
- (6) Hitchcock, P. B.; Lappert, M. F.; Maron, L.; Protchenko, A. V. Lanthanum Does Form Stable Molecular Compounds in the +2 Oxidation State. *Angew. Chem., Int. Ed.* **2008**, *47*, 1488–1491.
- (7) MacDonald, M. R.; Ziller, J. W.; Evans, W. J. Synthesis of a Crystalline Molecular Complex of Y^{2+} , [(18-Crown-6)K]-[(C_5H_4 SiMe $_3$) $_3$ Y]. J. Am. Chem. Soc. **2011**, 133, 15914–15917.
- (8) MacDonald, M. R.; Bates, J. E.; Fieser, M. E.; Ziller, J. W.; Furche, F.; Evans, W. J. Expanding Rare-Earth Oxidation State Chemistry to Molecular Complexes of Holmium(II) and Erbium(II). *J. Am. Chem. Soc.* **2012**, *134*, 8420–8423.
- (9) MacDonald, M. R.; Bates, J. E.; Ziller, J. W.; Furche, F.; Evans, W. J. Completing the Series of +2 Ions for the Lanthanide Elements: Synthesis of Molecular Complexes of Pr²⁺, Gd²⁺, Tb²⁺, and Lu²⁺. J. Am. Chem. Soc. **2013**, 135, 9857–9868.
- (10) Fieser, M. E.; MacDonald, M. R.; Krull, B. T.; Bates, J. E.; Ziller, J. W.; Furche, F.; Evans, W. J. Structural, Spectroscopic, and Theoretical Comparison of Traditional vs Recently Discovered Ln^{2+} Ions in the $[K(2.2.2\text{-Cryptand})][(C_5H_4SiMe_3)_3Ln]$ Complexes: The Variable Nature of Dy^{2+} and Nd^{2+} . *J. Am. Chem. Soc.* **2015**, *137*, 369–382.
- (11) Kotyk, C. M.; MacDonald, M. R.; Ziller, J. W.; Evans, W. J. Reactivity of the Ln^{2+} Complexes [K(2.2.2-Cryptand)]-[(C₃H₄SiMe₃)₃Ln]: Reduction of Naphthalene and Biphenyl. *Organometallics* **2015**, 34, 2287–2295.
- (12) Woen, D. H.; Chen, G. P.; Ziller, J. W.; Boyle, T. J.; Furche, F.; Evans, W. J. Solution Synthesis, Structure, and CO₂ Reduction

- Reactivity of a Scandium(II) Complex, $\{Sc[N(SiMe_3)_2]_3\}^-$. Angew. Chem., Int. Ed. **2017**, 56, 2050–2053.
- (13) Woen, D. H.; Chen, G. P.; Ziller, J. W.; Boyle, T. J.; Furche, F.; Evans, W. J. End-On Bridging Dinitrogen Complex of Scandium. *J. Am. Chem. Soc.* **2017**, *139*, 14861–14864.
- (14) Palumbo, C. T.; Fieser, M. E.; Ziller, J. W.; Evans, W. J. Reactivity of Complexes of 4fⁿ5d¹ and 4fⁿ⁺¹ Ln²⁺ Ions with Cyclooctatetraene. *Organometallics* **2017**, *36*, 3721–3728.
- (15) Trinh, M. T.; Wedal, J. C.; Evans, W. J. Evaluating Electrochemical Accessibility of $4f^n5d^1$ and $4f^{n+1}$ Ln(I) Ions in $(C_5H_4SiMe_3)_3Ln$ and $(C_5Me_4H)_3Ln$ Complexes. *Dalton Trans.* **2021**, *50*, 14384–14389.
- (16) Wedal, J. C.; Evans, W. J. A Rare-Earth Metal Retrospective to Stimulate All Fields. J. Am. Chem. Soc. 2021, 143, 18354—18367.
- (17) Meihaus, K. R.; Fieser, M. E.; Corbey, J. F.; Evans, W. J.; Long, J. R. Record High Single-Ion Magnetic Moments Through $4f^n5d^1$ Electron Configurations in the Divalent Lanthanide Complexes $[(C_5H_4SiMe_3)_3Ln]^-$. J. Am. Chem. Soc. **2015**, 137, 9855–9860.
- (18) Ariciu, A. M.; Woen, D. H.; Huh, D. N.; Nodaraki, L. E.; Kostopoulos, A. K.; Goodwin, C. A. P.; Chilton, N. F.; McInnes, E. J. L.; Winpenny, R. E. P.; Evans, W. J.; Tuna, F. Engineering Electronic Structure to Prolong Relaxation Times in Molecular Qubits by Minimising Orbital Angular Momentum. *Nat. Commun.* **2019**, *10*, 1–8.
- (19) Kundu, K.; White, J. R. K.; Moehring, S. A.; Yu, J. M.; Ziller, J. W.; Furche, F.; Evans, W. J.; Hill, S. A 9.2-GHz Clock Transition in a Lu(II) Molecular Spin Qubit Arising from a 3,467-MHz Hyperfine Interaction. *Nat. Chem.* **2022**, *14*, 392–397.
- (20) Jenkins, T. F.; Bekoe, S.; Ziller, J. W.; Furche, F.; Evans, W. J. Synthesis of a Heteroleptic Pentamethylcyclopentadienyl Yttrium(II) Complex, $[K(2.2.2\text{-}Cryptand)]\{(C_5Me_5)_2Y^{II}[N(SiMe_3)_2]\}$, and Its C-H Bond Activated Y(III) Derivative. *Organometallics* **2021**, *40*, 3917–3925.
- (21) Moore, W. N. G.; Ziller, J. W.; Evans, W. J. Optimizing Alkali Metal (M) and Chelate (L) Combinations for the Synthesis and Stability of $[M(L)][(C_5H_4SiMe_3)_3Y]$ Yttrium(II) Complexes. *Organometallics* **2021**, 40, 3170–3176.
- (22) Ryan, A. J.; Ziller, J. W.; Evans, W. J. The Importance of the Counter-Cation in Reductive Rare-Earth Metal Chemistry: 18-Crown-6 Instead of 2,2,2-Cryptand Allows Isolation of $[Y^{II}(NR_2)_3]^{1-}$ and Ynediolate and Enediolate Complexes from CO Reactions. *Chem. Sci.* **2020**, *11*, 2006–2014.
- (23) Meyer, G. Superbulky Ligands and Trapped Electrons: New Perspectives in Divalent Lanthanide Chemistry. *Angew. Chem., Int. Ed.* **2008**, 47, 4962–4964.
- (24) Huh, D. N.; Ciccone, S. R.; Bekoe, S.; Roy, S.; Ziller, J. W.; Furche, F.; Evans, W. J. Synthesis of Ln^{II}-in-Cryptand Complexes by Chemical Reduction of Ln^{III}-in-Cryptand Precursors: Isolation of a Nd^{II}-in-Cryptand Complex. *Angew. Chem., Int. Ed.* **2020**, *59*, 16141–16146.
- (25) Cloke, F. G. N. Zero Oxidation State Compounds of Scandium, Yttrium, and the Lanthanides. *Chem. Soc. Rev.* **1993**, *22*, 17–24.
- (26) Brennan, J. G.; Cloke, F. G. N.; Sameh, A. A.; Zalkin, A. Synthesis of $Bis(\eta\text{-}1,3,5\text{-}Tri\text{-}t\text{-}Butylbenzene})$ Sandwich Complexes of Yttrium(0) and Gadolinium(0); The X-Ray Crystal Structure of the First Authentic Lanthanide(0) Complex, $[Gd(\eta\text{-}But_3^t\text{C}_6\text{H}_3)_2]$. *J. Chem. Soc. Chem. Commun.* 1987, 1668–1669.
- (27) Anderson, D. M.; Cloke, F. G. N.; Cox, P. A.; Edelstein, N.; Green, J. C.; Pang, T.; Sameh, A. A.; Shalimoff, G. On the Stability and Bonding in $Bis(\eta$ -Arene)lanthanide Complexes. *J. Chem. Soc. Chem. Commun.* **1989**, 53–55.
- (28) Arnold, P. L.; Cloke, F. G. N.; Hitchcock, P. B.; Nixon, J. F. The First Example of a Formal Scandium(I) Complex: Synthesis and Molecular Structure of the 22-Electron Scandium Triple Decker Incorporating the Novel 1,3,5-Triphosphabenzene Ring. J. Am. Chem. Soc. 1996, 118, 7630–7631.
- (29) Fong, F. K.; Cape, J. A.; Wong, E. Y. Monovalent Samarium in Potassium Chloride. *Phys. Rev.* **1966**, *151*, 299–303.

- (30) Dieke, G. H. Divalent Rare Earth Ions in Crystals. *Spectra and Energy Levels of Rare Earth Ions in Crystals*; Interscience Publishers, 1968; Chapter 12, pp 177–188.
- (31) McClure, D. S.; Kiss, Z. Survey of the Spectra of the Divalent Rare-Earth Ions in Cubic Crystals. *J. Chem. Phys.* **1963**, 39, 3251–3257.
- (32) Qiu, J.; Hirao, K. γ -Ray Induced Reduction of Sm³⁺ to Sm²⁺ in Sodium Aluminoborate Glasses. *J. Mater. Sci. Lett.* **2001**, 20, 691–693.
- (33) Madhu, A.; Eraiah, B.; Srinatha, N. Gamma Irradiation Effects on the Structural, Thermal and Optical Properties of Samarium Doped Lanthanum—Lead- Boro-Tellurite Glasses. *J. Lumin.* **2020**, 221, 117080.
- (34) Telser, J.; Davydov, R.; Horng, Y. C.; Ragsdale, S. W.; Hoffman, B. M. Cryoreduction of Methyl-Coenzyme M Reductase: EPR Characterization of Forms, MCR_{ox1} and MCR_{red1}. *J. Am. Chem. Soc.* **2001**, *123*, 5853–5860.
- (35) Davydov, R.; Razeghifard, R.; Im, S. C.; Waskell, L.; Hoffman, B. M. Characterization of the Microsomal Cytochrome P450 2B4 $\rm O_2$ Activation Intermediates by Cryoreduction and Electron Paramagnetic Resonance. *Biochemistry* **2008**, 47, 9661–9666.
- (36) Davydov, R. M.; Chauhan, N.; Thackray, S. J.; Anderson, J. L. R.; Papadopoulou, N. D.; Mowat, C. G.; Chapman, S. K.; Raven, E. L.; Hoffman, B. M. Probing the Ternary Complexes of Indoleamine and Tryptophan 2,3-Dioxygenases by Cryoreduction EPR and Endor Spectroscopy. J. Am. Chem. Soc. 2010, 132, 5494–5500.
- (37) Davydov, R. M.; McLaughlin, M. P.; Bill, E.; Hoffman, B. M.; Holland, P. L. Generation of High-Spin Iron(I) in a Protein Environment Using Cryoreduction. *Inorg. Chem.* **2013**, *52*, 7323–7325.
- (38) Dickinson, L. C.; Symons, M. C. R. Electron Spin Resonance Monitoring of Ligand Ejection Reactions Following Solid-State Reduction of Cobalt Globin and Cobalt Protoporphyrin Complexes. *J. Phys. Chem.* **1982**, *86*, 917–921.
- (39) Konishi, S.; Hoshino, M.; Imamura, M. Formation of the Charge-Transfer and Constrained Complexes of Cobalt(II) Tetraphenylporphyrin in Rigid Solution. *J. Phys. Chem.* **1980**, 84, 3437–3440.
- (40) Edelmann, F. T. Synthetic Methods of Organometallics and Inorganic Chemistry; Herrmann, W. A., Ed.; Thieme Verlag Stuttgart: New York, 1997; Vol. 6, pp 37–40.
- (41) Peterson, J. K.; MacDonald, M. R.; Ziller, J. W.; Evans, W. J. Synthetic Aspects of $(C_5H_4SiMe_3)_3Ln$ Rare-Earth Chemistry: Formation of $(C_5H_4SiMe_3)_3Lu$ via $[(C_5H_4SiMe_3)_2Ln]^+$ Metallocene Precursors. *Organometallics* **2013**, *32*, 2625–2631.
- (42) Jou, F. Y.; Dorfman, L. M. Pulse Radiolysis Studies. XXI. Optical Absorption Spectrum of the Solvated Electron in Ethers and in Binary Solutions of These Ethers. *J. Chem. Phys.* **1973**, *58*, 4715–4723.
- (43) Fang, M.; Lee, D. S.; Ziller, J. W.; Doedens, R. J.; Bates, J. E.; Furche, F.; Evans, W. J. Synthesis of the $(N_2)^{3-}$ Radical from Y^{2+} and Its Protonolysis Reactivity To Form $(N_2H_2)^{2-}$ via the Y[N- $(SiMe_3)_2]_3/KC_8$ Reduction System. J. Am. Chem. Soc. **2011**, 133, 3784–3787.
- (44) Ryan, A. J.; Darago, L. E.; Balasubramani, S. G.; Chen, G. P.; Ziller, J. W.; Furche, F.; Long, J. R.; Evans, W. J. Synthesis, Structure, and Magnetism of Tris(Amide) [Ln{N(SiMe₃)₂}₃]¹⁻ Complexes of the Non-Traditional +2 Lanthanide Ions. *Chem. A Eur. J.* **2018**, *24*, 7702–7709.
- (45) Staroverov, V. N.; Scuseria, G. E.; Tao, J.; Perdew, J. P. Comparative Assessment of a New Nonempirical Density Functional: Molecules and Hydrogen-Bonded Complexes. *J. Chem. Phys.* **2003**, 119, 12129–12137.
- (46) Grimme, S.; Antony, J.; Ehrlich, S.; Krieg, H. A Consistent and Accurate Ab Initio Parametrization of Density Functional Dispersion Correction (DFT-D) for the 94 Elements H-Pu. *J. Chem. Phys.* **2010**, 132, 154104.
- (47) Grimme, S. Semiempirical GGA-Type Density Functional Constructed with a Long-Range Dispersion Correction. *J. Comput. Chem.* **2006**, 27, 1787–1799.

- (48) Weigend, F.; Köhn, A.; Hättig, C. Efficient Use of the Correlation Consistent Basis Sets in Resolution of the Identity MP2 Calculations. *J. Chem. Phys.* **2002**, *116*, 3175–3183.
- (49) Weigend, F.; Ahlrichs, R. Balanced Basis Sets of Split Valence, Triple Zeta Valence and Quadruple Zeta Valence Quality for H to Rn: Design and Assessment of Accuracy. *Phys. Chem. Chem. Phys.* **2005**, *7*, 3297–3305.
- (50) Eichkorn, K.; Weigend, F.; Treutler, O.; Ahlrichs, R. Auxiliary Basis Sets for Main Row Atoms and Transition Metals and Their Use to Approximate Coulomb Potentials. *Theor. Chem. Acc.* **1997**, *97*, 119–124.
- (51) Schäfer, A.; Klamt, A.; Sattel, D.; Lohrenz, J. C. W.; Eckert, F. COSMO Implementation in TURBOMOLE: Extension of an Efficient Quantum Chemical Code towards Liquid Systems. Phys. Chem. Chem. Phys. 2000, 2, 2187–2193.
- (52) CRC Handbook of Chemistry and Physics, 97th ed.; Haynes, W. M., Lide, D. R., Bruno, T. J., Eds.; CRC Press, 2016.
- (53) Jenkins, T. F.; Woen, D. H.; Mohanam, L. N.; Ziller, J. W.; Furche, F.; Evans, W. J. Tetramethylcyclopentadienyl Ligands Allow Isolation of Ln(II) Ions across the Lanthanide Series in $[K(2.2.2-Cryptand)][(C_5Me_4H)_3Ln]$ Complexes. *Organometallics* **2018**, 37, 3863–3873.
- (54) Wedal, J. C.; Furche, F.; Evans, W. J. Density Functional Theory Analysis of the Importance of Coordination Geometry for 5f³6d¹versus 5f⁴Electron Configurations in U(II) Complexes. *Inorg. Chem.* **2021**, *60*, 16316–16325.
- (55) Wedal, J. C.; Ziller, J. W.; Furche, F.; Evans, W. J. Synthesis and Reduction of Heteroleptic Bis(Cyclopentadienyl) Uranium(III) Complexes. *Inorg. Chem.* **2022**, *61*, 7365–7376.
- (56) TURBOMOLE V7.4.1 2019, University of Karlsruhe and Forschungszentrum Karlsruhe GmbH, 1989–2007, TURBOMOLE GmbH, 2007, Available from http://www.turbomole.com.
- (57) Balasubramani, S. G.; Chen, G. P.; Coriani, S.; Diedenhofen, M.; Frank, M. S.; Franzke, Y. J.; Furche, F.; Grotjahn, R.; Harding, M. E.; Hättig, C.; Hellweg, A.; Helmich-Paris, B.; Holzer, C.; Huniar, U.; Kaupp, M.; Marefat Khah, A.; Karbalaei Khani, S.; Müller, T.; Mack, F.; Nguyen, B. D.; Parker, S. M.; Perlt, E.; Rappoport, D.; Reiter, K.; Roy, S.; Rückert, M.; Schmitz, G.; Sierka, M.; Tapavicza, E.; Tew, D. P.; van Wüllen, C.; Voora, V. K.; Weigend, F.; Wodyński, A.; Yu, J. M. TURBOMOLE: Modular Program Suite for Ab Initio Quantum-Chemical and Condensed-Matter Simulations. *J. Chem. Phys.* 2020, 152, 184107.